Title: Effects of Interleukin-6 dysregulation in a mouse model of Alzheimer's disease: unraveling the complexity beyond amyloidosis

Authors: Carla Canal [1,2], Kevin Aguilar [1,2,3], Gemma Comes [1,2], Paula Sanchis [1,2,4] Amalia Molinero [1,2], Mercedes Giralt [1,2], Juan Hidalgo* [1,2]

Authors affiliation:

[1] Department of Cell Biology, Physiology, and Immunology, Animal Physiology Unit, Faculty of Biosciences, Universitat Autònoma de Barcelona, Bellaterra, Barcelona, Spain.

[2] Institut de Neurociències, Universitat Autònoma de Barcelona, Bellaterra, Barcelona, Spain.

[3] Current affiliation: Institute for Research in Biomedicine (IRB Barcelona), Barcelona, Spain.

[4] Current affiliation: Centre of Inflammation and Metabolism/Centre for Physical Activity Research (CIM/CFAS), Rigshospitalet, University of Copenhagen, Copenhagen, Denmark.

Keywords: Alzheimer's disease (AD), Interleukin-6 (IL-6), Tg2576, Amyloid precursor protein (APP), amyloid-β peptides (Aβ), neuroinflammation, glial reactivity.

Correspondence: Juan Hidalgo, Department of Cellular Biology, Physiology and Immunology, Animal Physiology Unit, Faculty of Biosciences, Universitat Autònoma de Barcelona, Barcelona 08193, Spain. Email: Juan.Hidalgo@uab.es

1. Abstract

Interleukin-6 dysregulation has been implicated in the pathological progression of Alzheimer's disease (AD), a leading cause of dementia in the ageing population. Here we show that chronic neuroinflammation elicited by transgenic expression of IL-6 and systemic IL-6 deficiency influences the phenotype of the Tg2576 mouse model of AD, modulating mortality, body weight, behavioral and cognitive traits, amyloidosis, and neuroinflammation. While the conventional understanding of AD pathophysiology emphasizes the central role of Aβ peptides and amyloid plaques in the development and progression the disease, the absence of amyloidosis in the brain in a specific subset of Tg2576 mice challenges this notion. This suggests that several Tg2576-related traits may manifest independently of Aβ, pointing to a potential contribution of alternative APP-related factors or pathways to the phenotypic alterations observed in Tg2576 mice. Together, our findings underscore the complexity of AD pathogenesis and emphasize the multifaceted nature of IL-6 in both physiological and neurodegenerative processes, particularly in the context of AD.

2. Introduction

Alzheimer's disease (AD) stands as the primary cause of dementia among the elderly, with no significant breakthroughs in the discovery of effective disease-modifying treatments despite extensive research efforts over recent decades (1). The formation of extracellular amyloid deposits of amyloid-β peptides (Aβ) and intracellular neurofibrillary tangles of hyperphosphorylated tau protein, are the two main histopathological hallmarks of AD, predominantly affecting brain regions as the hippocampus and the cortex. Extensive neuronal dysfunction, synaptic loss, vascular damage, and neuroinflammation have also been related to the pathophysiology of the disease (2). Indeed, the inflammatory response to Aβ has been directly associated with the development and pathogenesis of AD. This response involves glial reactivity and the release of inflammatory mediators, likely serving as a defense mechanism to contain Aβ peptides accumulation and regulate the local microenvironment. However, glial reactivity also activates the production and processing of APP leading to sustained elevated levels of Aβ, ultimately contributing to disease progression and severity (3–7).

Interleukin-6 (IL-6) is a pleiotropic cytokine with pro- and anti-inflammatory effects. Ever since its discovery, a significant role for IL-6 in the CNS emerged, and its dysregulation has been associated to the pathological process of AD (8). In fact, IL-6 levels are increased in the serum and brain tissue of AD patients, especially in the area surrounding senile plaques and in the cerebrospinal fluid (7,9). In addition, IL-6 along with other pro-inflammatory cytokines such as IL-1β and TNF-α, are also able to promote amyloid precursor protein (APP) production and enhance BACE1 levels and activity, a critical enzyme in APP cleavage to Aβ, resulting in a self-reinforcing positive feedback loop in AD pathogenesis (7,10). The upregulation of IL-6 is also observed in AD translational mouse models, in which IL-6 is present both around and within β-amyloid plaques (11).

A frequently used and well-characterized transgenic model is the Tg2576 mouse model, which overexpresses human APP (hAPP) harboring the Swedish two-point mutation KM670/671NL (12). This model displays early and aging-associated behavioral and cognitive impairments and pathophysiological features that include Aβ oligomer formation and aggregation into extracellular amyloid deposits, neuritic dystrophy, and neuroinflammation (12–15). However, the mechanisms underlying the effects of hAPP overexpression in Tg2576 are still to be fully elucidated, as recent

evidence highlights that molecular perturbance and cognitive impairments may occur independently of Aβ formation (16). In mice, the formation of soluble Aβ and other fragments require transgenic expression of hAPP. Thus, the specific patterns of transgene expression may contribute to specific pathological and cognitive disturbances observed in Tg2576 mice before amyloid plaque pathology becomes apparent, rather resulting from altered APP signaling than of Aβ toxicity (17,18).

Given the potential role of IL-6 in modulating behavior previously demonstrated in both IL-6 overexpressing mice and IL-6 deficient mice (19–22), we hypothesized that IL-6 could play a critical role modulating the phenotype of Tg2576 mice. Furthermore, IL-6 could influence the molecular pathways of Aβ formation and aggregation. Indeed, evidence suggests a protective role for IL-6 by promoting gliosis, which reduces Aβ deposition and promotes plaque clearance through phagocytosis (5,23–25). Here we provide new insights into the impact of IL-6 on the phenotype of Tg2576 mice in two main paradigms: chronic neuroinflammation elicited by transgenic expression of IL-6 in astrocytes and systemic IL-6 deficiency. Our findings elucidate a complex interaction between IL-6 and the phenotype of Tg2576 mice, highlighting a potential role for IL-6 in AD development and progression. This study also challenges the conventional understanding of the role of Aβ peptides in Tg2576 mice and underscores the importance of reevaluating existing paradigms in animal models.

3. Materials and methods

3.1. Animals

Tg2576 mice (Taconic Europe) (12), GFAP-IL6 mice (26), and IL-6-DIO-KO mice (27) were used in this study. Hemizygous Tg2576 male mice were bred with hemizygous GFAP-IL6 mice to generate WT (*hAPP*$^{+/+}$, Gfap-Il6$^{+/+}$), GFAP-IL6 (*hAPP*$^{+/+}$, Gfap-Il6$^{Tg/+}$), Tg2576 (*hAPP*$^{Tg/+}$, Gfap-Il6$^{+/+}$), and Tg2576/GFAP-IL6 (*hAPP*$^{Tg/+}$, Gfap-Il6$^{Tg/+}$). Also, hemizygous Tg2576 mice were bred with homozygous IL-6-DIO-KO mice following a two-step breeding strategy to generate control (*hAPP*$^{+/+}$, *Il6*$^{+/+}$), referred to as WT in the text, IL6KO (*hAPP*$^{+/+}$, *Il6*$^{\Delta/+}$), Tg2576 (*hAPP*$^{Tg/+}$, *Il6*$^{+/+}$), and Tg2576/IL6KO (*hAPP*$^{Tg/+}$, *Il6*$^{\Delta/+}$). Genotype was determined by PCR analysis as previously described (26–28). Mice were group-housed with littermates in a temperature-controlled environment (22 ± 2 ºC) under specific pathogen-free conditions, with a 12-hour dark-light cycle and were maintained with food and water available *ad libitum*. Experiments were conducted during the light

137 phase and mice were monitored regularly from weaning to euthanasia at 18 months
138 of age. Both male and female mice were used unless otherwise noted. All
139 experimental protocols were approved by the Ethics Committee on Animal and
140 Human Experimentation (CEEAH) of the Autonomous University of Barcelona (3971
141 and 9861) and were conducted in accordance with the Spanish legislation and the
142 EU directive (2010/63/UE) on 'Protection of Animals Used for Experimental and
143 Other Scientific Purposes'.

144 *3.2. Behavioral tests*

145 Behavioral evaluation was performed at 5-6 (young) and at 16–17 (old) months of
146 age, akin to methodology previously described (29,30). Mice were handled for 5 days
147 before testing for habituation, and a 30-minute acclimation in the home cage within
148 the testing room preceded each test. Tests were conducted in the following order on
149 alternate days: open field (OF), hole board (HB), elevated plus maze (EPM), pole
150 test, Y-maze (YM) and/or Morris water maze (MWM), and nesting. Behavioral data
151 collection and analyses were performed under blind conditions.

152 *3.2.1. OF, HB, and EPM tests*

153 Locomotor and exploratory activity were assessed in an OF. Mice were placed in a
154 rectangular apparatus (36,5 x 56 x 31 cm) and allowed to freely explore it for 5 min.
155 The measured parameters were total horizontal activity (ambulatory distance) and
156 counts for vertical activity (rearings).

157 Exploratory behavior was assessed in a HB. Mice were placed in a square
158 apparatus (40 x 40 x 21,5 cm) with four equally spaced bottom holes (3 cm diameter)
159 and allowed to freely explore it for 5 min. The measured parameters were the time
160 and number of head-dipping events.

161 Anxiety-like behavior was assessed in an EPM. Mice were placed in a cross-
162 shaped maze consisting of two open arms (20 x 5 cm) and two closed arms (20 x 5 x
163 15 cm) elevated 47 cm from the floor and were allowed to freely explore the
164 apparatus for 5 min. The measured parameters were percentage of entries and time
165 spent in the open arms (OA) of the apparatus (excluding the center).

166 *3.2.2. Pole test*

167 Motor coordination and balance of mice were evaluated using the pole test. Mice
168 were placed head-up on top of a vertical pole (30 cm height, 1 cm diameter) with a
169 rough surface for 120 sec at maximum. Mice underwent three trials of habituation
170 one week before testing. On test day, three consecutive trials were conducted with a

171 10-min separation, and the time to descend (maximum duration was scored if the
172 mouse fell down the pole) and the number of failed trials were measured.

173 *3.2.3. YM and MWM tests*

174 A Y-Maze was used to assess working and spatial reference memory. Mice were
175 placed at the starting arm of a Y-shaped maze consisting of three closed arms (33 x
176 5 x 15 cm) with external cues placed around the apparatus. To assess working
177 memory, mice were allowed to freely explore the apparatus in a single 8-min trial.
178 Arm entries and alternations (three consecutive entries to three different arms) were
179 calculated as alternations / (total arm entries – 2) * 100. To assess spatial reference
180 memory, mice were allowed to freely explore the apparatus for 10 min with one arm
181 closed off (training session), and after 1 and 2 h the blocker was removed, and mice
182 were allowed to explore the apparatus for 5 min (trial sessions). The measured
183 parameters were entries and time spent in the novel arm (NA) of the apparatus.

184 The MWM was used to assess learning and spatial memory. The apparatus
185 consisted of a round pool (120 cm diameter x 60 cm deep) virtually divided into four
186 equal quadrants with a removable platform (8 cm diameter). The pool was filled with
187 opaque water at 22 ± 1 ºC and surrounded by external cues for spatial references.
188 Animals were tested for 11 days in differentiated phases as in the following protocol
189 (30). Briefly, animals were challenged to escape from the pool by finding the hidden
190 platform (submerged 1 cm) in a target quadrant (TQ). Four-trial sessions (1 min
191 each) during four consecutive days were performed. The platform was removed and
192 short- (1 hour after the last training session) and long-term memory (24 hours after)
193 were tested in the probe trials (30 sec each). The evaluation included both spatial
194 acquisition and spatial reversal (re-learning of a new platform location) phases. The
195 measured parameters include escape latency (time to find the hidden platform, mean
196 of four trials) and area under the curve (AUC) calculated for each the training curve,
197 and latency to reach the platform area (PA) in the probe trials.

198 *3.2.4. Nesting behavior*

199 Natural behavior of mice was assessed with the nesting behavior test. During the
200 testing period, nesting mice were individually housed, and 3 g of nesting material
201 (Nestlet) were provided 1 h before the onset of the dark cycle. Nests were assessed
202 1 h after the next light cycle started and nesting scores were calculated by the extent
203 of shredded material and the shape of the nest constructed on a scale of 1-5 (from

204 undisturbed material to near perfect nest) according to published criteria (31). Only
205 female mice were included in the study.
206 *3.2.5.* Analysis of behavior
207 Tests were recorded by an overhead video camera and videos were analyzed with
208 either the Ethovision program version 11 (OF, HB, EPM, and YM) or the ANY-maze
209 version 5.1 (MWM). Data was obtained through both *in situ* manual measurements
210 and automatic tracking analysis.
211 *3.3. Neuropathological analysis*
212 *3.3.1. Sample collection*
213 Mice were weighed and killed by decapitation at 18 months of age. Whole
214 blood was collected, allowed to clot, and centrifuged at 6000 x g for 10 min at 4 ºC to
215 separate serum samples. Brains were extracted and the left hemisphere was fixed in
216 4% paraformaldehyde (PFA) for 24 h at 4 ºC for further processing. The right
217 hemisphere was dissected into cortex (anterior and posterior) and hippocampus and
218 rapidly frozen in liquid nitrogen and stored at -80 ºC for subsequent analysis.
219 *3.3.2. Western Blot*
220 Samples were homogenized by sonication in a lysis buffer (50 mM Tris-HCl pH
221 7.6, 150 mM NaCl, 2mM EDTA, 0,1% Igepal CA 630, 3% SDS, and 2% sodium
222 deoxycholate, supplemented with a protease inhibitor cocktail and
223 phenylmethylsulfonyl fluoride). Total tissue protein quantification was performed with
224 the Pierce™ BCA Protein Assay Kit (ThermoFisher) according to the manufacturer's
225 protocol.
226 Cortical and hippocampal lysates were prepared in NuPAGE™ LDS 4X (Invitrogen
227 NP0008) and 2-mercaptoethanol (Sigma-Aldrich 805740) and were heat shock for 5
228 min at 90 ºC. Proteins were separated by electrophoresis on a NuPage™ 4–12% Bis-
229 Tris Midi protein Gel (Invitrogen) and transferred to 0,2 µm nitrocellulose membranes.
230 Membranes were blocked with 5% (w/v) skim milk and incubated with primary
231 antibodies (mouse anti-β-amyloid$_{1-16}$ 6E10 1:2000, 803003 Biolegend; rabbit anti-
232 GFAP 1:40000, Z0334 Dako; and rabbit anti-Iba-1 1:3000, 019-19741 Wako)
233 overnight at 4 ºC, and with secondary antibodies (polyclonal rabbit anti-mouse
234 Ig/HRP 1:5000, P0260 Dako; and goat anti-rabbit IgG (H+L)-HRP conjugate 1:5000
235 and 1:10000, 1706515 Bio-Rad). Imunoreactive bands were detected using the
236 Clarity Western ECL Substrate (Bio-Rad), imaged in the Chemidoc Imaging System
237 (Bio-Rad), and analyzed using Image Lab™ 6.0 Software (Bio-Rad). Monoclonal anti-

238 β-Actin (1:5000, Sigma-Aldrich) was used as a loading control following membrane
239 stripping with 2% SDS, Tris HCl, and Tris Base pH 6.7.

240 *3.3.3. Enzyme-Linked ImmunoSorbent assay (ELISA)*

241 ELISA assay was performed to measure $A\beta_{40}$ and $A\beta_{42}$ (Amyloid beta 40 and 42
242 Human ELISA Kits, ThermoFisher) in cortical and hippocampal homogenates (as
243 described in 3.3.2) and in serum samples. The protocol was performed according to
244 the manufacturer's recommendations. The protein concentration of the lysate was
245 used to normalize the data.

246 *3.3.4. Immunofluorescence (IF)*

247 Fixed tissues were frozen in OCT, and tissue was sagittally cut into serial 20-µm-
248 thick sections in a cryostat (Leica CM3050 S). All the procedures in this subsection
249 were performed in free-floating sections. Sections were blocked with 1% BSA in
250 PBS-Triton 0,2%. For amyloid plaques detection, a 5-minute pre-treatment with 70%
251 formic acid was performed. Sections were incubated with primary antibodies (mouse
252 anti-β-amyloid$_{17\text{-}24}$ 4G8, Biolegend; rabbit anti-GFAP, Dako; and rabbit anti-IBA-1,
253 Wako) at 1:500 in blocking solution, and then with secondary antibodies (goat anti-
254 mouse IgG (H+L) Alexa Fluor™ 488 1:600; Invitrogen A11001; and donkey anti-
255 rabbit IgG (H+L) Alexa Fluor™ 594 1:600; Invitrogen A21207) in blocking solution.
256 Slices were mounted and covered with DAPI Fluoromount-G® mounting media
257 (Southern Biotech 0100-20). For quantification, three non-consecutive sections per
258 mouse were selected and imaged using an EVOS™ M5000 Imaging System
259 (Invitrogen) microscope, and images were analyzed using ImageJ software (32). The
260 sum of intensity of the specific signal (integrated density) was determined for cortex
261 and hippocampus and normalized by the area of the region of interest (Area ROI).
262 The integrated density values for GFAP and Iba1 surrounding amyloid plaques were
263 also quantified and normalized by Area ROI (plaque-shaped areas).

264 *3.4. Statistics*

265 Data are shown as mean ± SEM and plotted using GraphPad Prism version 10.
266 Statistical analysis was conducted using SPSS version 23 with separate analyses
267 performed for male and female samples. Survival was evaluated using the Kaplan-
268 Meier and Log-rank survival tests, with genotype as a four-level factor. Data with two
269 variables to compare was analyzed either with a Generalized Linear Model (GzLM)
270 with both genotypes as main factors and appropriate post hoc pairwise comparisons
271 when needed (sequential Bonferroni's correction), or with Generalized Estimated

272 Equations (GEE) for repeated measures, including both genotypes as main factors
273 and time as a within-subject factor. Statistical significance was set as $p \leq 0.05$.
274 Sample size is stated in the text or figure as needed.
275
276 **4. Results**
277 *4.1. IL-6 impacts on the mortality and body weight loss observed in AD-like*
278 *Tg2576 mice in a sex-dependent manner*
279 Survival was significant decreased in both male and female Tg2576 mice **(Fig.**
280 **1A, B)**. IL-6 overexpression aggravated Tg2576-associated mortality in female mice,
281 and the same trend was observed in male mice. Conversely, a pro-survival trend was
282 observed in male GFAP-IL6 mice, while minimal mortality was observed in female
283 mice **(Fig. 1A)**. IL-6 deficiency partially rescued the mortality observed in female
284 Tg2576 mice, but not in males. Interestingly, both male and female IL6KO mice also
285 experienced reduced survival **(Fig. 1B)**.
286 Tg2576 animals also exhibited lower body weight throughout lifetime compared
287 to littermate controls **(Fig. 1C, D)**. Transgenic expression of IL-6 resulted in late-
288 onset decreased body weight in females, especially in GFAP-IL6 mice, but not in
289 males **(Fig. 1C)**. In contrast, IL6KO males developed mature-onset obesity, as
290 evidenced by increased body weight compared to WT littermates, but not in females
291 **(Fig. 1D)**.
292 4.2. *IL-6 modulates AD-like behavior parameters in Tg2576 mice from early stages*
293 Young Tg2576 (5-6 months old) mice exhibited hyperactivity in the OF test,
294 characterized by increased ambulation and rearing behaviors (horizontal and vertical
295 activity, respectively), enhanced exploratory behavior in the HB, as revealed by an
296 increased time and frequency of head-dipping events, and decreased anxiety in the
297 EPM, shown by an increased percentage of entries and time spent in the open arms
298 of the maze. Notably, these changes were predominantly observed in females **(Fig.**
299 **2A-F)**. In male GFAP-IL6 mice, particularly Tg2576/GFAP-IL6 mice, increased
300 vertical and horizontal activity was noted compared to littermate controls. In contrast,
301 the opposite trend was observed in female mice **(Fig. 2A)**. Similarly, IL-6
302 overexpression increased exploratory behavior in male Tg2576 mice **(Fig. 2B)**.
303 Additionally, both male and female IL-6-overexpressing mice exhibited reduced
304 anxiety-like behavior, particularly in Tg2576/GFAP-IL6 mice **(Fig. 2C)**. In contrast, IL-

305 6 deficiency reversed the hyperactive phenotype in Tg2576/IL6KO mice but did not
306 affect their exploratory or anxiety behaviors. Notably, no clear-cut effects were
307 observed in IL6KO mice when compared to WT mice in these behavioral tests **(Fig.**
308 **2D-F)**.
309 In aged Tg2576 mice (16-17 months old), behavioral impairments similar to those
310 observed in young mice persisted **(Fig. 3A-F)**. In contrast to the findings in young
311 mice, IL-6 overexpression in aged mice reversed hyperactivity in both sexes **(Fig.**
312 **3A)** and partially restored exploratory behavior in Tg2576/GFAP-IL6 females while
313 increasing it in males **(Fig. 3B)**. Additionally, IL-6 overexpression increased
314 frequency and duration in the OA of the EPM particularly in Tg2576/GFAP-IL6 female
315 mice, and male mice followed a similar trend **(Fig. 3C)**. Similarly, IL-6 deficiency
316 reversed hyperactivity in Tg2576 females, reducing both vertical and horizontal
317 activity **(Fig. 3D)**, but also the increased exploratory behavior in both males in
318 females **(Fig. 3E)**. Moreover, decreased anxiety in Tg2576 was modulated in a sex-
319 dependent manner by IL-6 deficiency, as it potentiated it in Tg2576/IL6KO females,
320 while it reversed it in male mice **(Fig. 3F)**. As in young mice, there were no significant
321 effects in IL6KO mice compared to WT mice in these behavioral tests, except for
322 anxiety in male mice, which was increased in IL6KO mice **(Fig. 3D-F)**.
323 A decline in motor performance was observed in aged Tg2576 mice, especially in
324 females, as evidenced by a significant increase in the time to descend from the pole
325 test, although not in the number of failed trials. GFAP-IL6 mice also displayed
326 impaired motor performance, characterized by an increased time to descend from the
327 pole, along with a higher number of failed trials. However, the effects of motor
328 impairment on Tg2576 mice were not compounded by IL-6 overexpression **(Fig. 3G)**.
329 Impaired nest-building behavior was observed in female Tg2576 mice, as
330 indicated by a decrease in average nesting scores that persisted through aging.
331 While IL-6 deficiency did not significantly influence this phenotype in Tg2576/IL6KO
332 mice, it was enhanced in IL6KO mice compared to WT littermates, especially at aged
333 stages **(Fig. 3H)**.
334 4.3. *IL-6 influences learning and memory impairment of Tg2576 mice*
335 Working memory was impaired in aged Tg2576 mice, displayed by a decrease in
336 the percentage of spontaneous alternations in the YM **(Fig. 4A, B)**. IL-6
337 overexpression improved working memory in both GFAP-IL6 and Tg2576/GFAP-IL6

338 female mice; in male mice, the same was observed in Tg2576/GFAP-IL6, but the
339 contrary in GFAP-IL6 animals. While a higher number of total arm entries was also
340 observed in Tg2576 mice, no effects were related to IL-6 overexpression **(Fig. 4A)**. In
341 contrast, IL-6 deficiency did not ameliorate working memory of Tg2576/IL6KO mice
342 **(Fig. 4B)**.
343 Spatial learning and memory were also impaired in aged Tg2576 mice, as
344 evidenced by a decreased percentage of time and entries to the novel arms of the
345 YM test in both sexes **(Fig. 4C)**, as well as an increase in the escape latency curves
346 and in the latency to the platform area of the MWM test, especially in males but not in
347 females **(Fig. 4D, E)**. IL-6 overexpression had opposite effects in females, as it
348 improved memory in GFAP-IL6 mice while worsening it in Tg2576/GFAP-IL6 mice,
349 particularly during the test performed 2 hours after training. Conversely, GFAP-IL6
350 male mice displayed worsened spatial memory **(Fig. 4C)**. IL-6 deficiency improved
351 learning in females, as seen by a reduction in escape latency and AUC, as well as
352 decreased latency to PA in both spatial acquisition and reversal phases. Similarly, IL-
353 6 deficiency tends to reverse the impaired memory in Tg2576 male mice in the
354 spatial reversal phase **(Fig. 4D, E)**.
355 *4.4. IL-6 regulates APP-related molecular pathways of Tg2576 mice*
356 The brains of Tg2576 mice are characterized by significant Aβ pathology and
357 progressive development of diffuse and senile plaque resulting from hAPP
358 overexpression and processing. As expected, amyloid plaques were present in
359 Tg2576 animals, as revealed by 4G8 immunostaining performed in the IL-6
360 overexpression study. Quantitative analysis indicated that amyloid plaques tend to be
361 increased in Tg2576/GFAP-IL6 mice compared to littermate Tg2576 mice **(Fig. 5A)**.
362 Western blot analysis revealed elevated levels of hAPP holoprotein and total Aβ
363 peptides in the cortex and hippocampus of Tg2576 mice, whereas, as expected, they
364 were absent in their wild type littermates. IL-6 overexpression decreased total Aβ
365 peptides levels in the cortex and hippocampus of Tg2576 mice. Likewise, a similar
366 trend was observed for APP levels **(Fig. 5B)**. ELISA analysis of specific Aβ species
367 revealed that IL-6 overexpression increased $A\beta_{42}$ levels, the most pathogenic form,
368 while decreasing the levels of $A\beta_{40}$ in both cortex and hippocampus. Therefore, a
369 dramatic shift in the $A\beta_{42}$ / $A\beta_{40}$ ratio was observed in Tg2576/GFAP-IL6 mice
370 compared to Tg2576 mice **(Fig. 5C)**.

371 In the IL-6 deficiency study, elevated levels of hAPP holoprotein were observed
372 again by Western Blot in the cortex and hippocampus of Tg2576 mice as compared
373 to wild type littermates. In contrast, we did not detect any Aβ proteolytic fragments in
374 the Tg2576 mice **(Fig. 5D)**. Similar results were found when assessing cortical and
375 hippocampal $A\beta_{40}$ and $A\beta_{42}$ levels by ELISA **(Fig. 5E)**. Control Tg2576 run in parallel
376 showed similar APP levels, which were normally processed rendering elevated Aβ
377 levels **(**blue bar in **Fig. 5D and E)**. In contrast to the results in the brain, $A\beta_{40}$ and
378 $A\beta_{42}$ were detected in Tg2576 serum samples, and these levels were significantly
379 decreased by IL-6 deficiency. Interestingly, Tg2576 mice, heterozygous for IL-6,
380 showed lower levels of Aβ peptides than positive controls, homozygous for IL-6 **(Fig.**
381 **5F)**.
382 4.5. *IL-6 modulates astrogliosis and microgliosis in Tg2576 mice*
383 Elevated levels of GFAP and Iba-1 were detected by Western Blot in cortical and
384 hippocampal homogenates of Tg2576 mice compared to littermate controls.
385 Increased levels of both markers were also observed in the cortex and hippocampus
386 of IL-6-overexpressing mice, especially in the hippocampus of IL-6-deficient mice.
387 There was a general sex- and area-dependent trend to an additive effect in the
388 double transgenic mice **(Fig. 6A, B).**
389 Quantification of GFAP immunostaining also showed increased astrogliosis in the
390 cortex and hippocampus of both Tg2576 and GFAP-IL6 mice compared to WT
391 littermates. In Tg2576/GFAP-IL6 mice, GFAP immunostaining was similar to that of
392 Tg2576 in both brain areas **(Fig. 7A, B)**. Quantification of Iba-1 immunostaining area
393 also revealed increased microgliosis in both cortex and hippocampus of female
394 Tg2576 mice, while no significant effects were observed in males. IL-6
395 overexpression dramatically increased Iba-1 levels in both brain areas and in both
396 sexes, but interestingly, and in contrast to GFAP, Tg2576/GFAPIL6 mice showed
397 similar Iba-1 immunostaining levels as GFAP-IL6 mice **(Fig. 7D, E)**. We next further
398 analyzed GFAP and Iba-1 immunostaining surrounding amyloid plaques, which
399 revealed distinct patterns in Tg2576 and Tg2576/GFAP-IL6 mice. In the former,
400 astrocytosis was predominantly localized around amyloid plaques, whereas in the
401 latter this was lower in both brain areas **(Fig. 7C)**. Similar results were observed for
402 microgliosis, as Iba-1 immunostaining associated with plaques in Tg2576 mice was
403 higher as compared to Tg2576/GFAP-IL6 mice **(Fig. 7F)**.
404

405 **5. Discussion**

406 Neuroinflammation plays a key role in the pathogenesis of AD disease, and
407 emerging data suggests that IL-6 is closely related to the development and
408 progression of the disease (9,11,33). Here, we elucidate that IL-6 has a significant
409 impact on various physiological, behavioral, and molecular aspects of the Tg2576
410 mouse model. Moreover, our study suggests that these effects may be independent
411 of APP processing and could rather be explained by APP overexpression than Aβ
412 formation and deposition.

413 Premature mortality was observed in both male and female Tg2576 mice
414 compared to their respective controls, as expected. Correlation studies indicate that
415 the underlying mechanisms for Tg2576 mortality may be partly attributed to Aβ
416 toxicity. Hence, preventing Aβ production or enhancing its clearance from the brain
417 can decrease mortality in mice (34). Nevertheless, the impact of APP on premature
418 mortality may extend beyond the well-established amyloid-related pathology
419 associated with AD, including potential factors such as seizures, cerebrovascular
420 dysfunctions, oxidative stress, genetic background, environmental factors, and sex-
421 dependent effects (28,35–38). IL-6 may be involved in several of these factors, as
422 evidenced by its role in maintaining BBB integrity and modulating neuronal
423 responses (39). In our study, IL-6 overexpression in astrocytes increased Tg2576-
424 induced mortality, while IL-6 deficiency rescued it, thus underscoring the crucial role
425 of this cytokine in the pathophysiology of the disease. This aligns with results from
426 studies inhibiting IL-6 trans-signaling, a crucial signaling pathway implicated in the
427 neuroinflammatory response of IL-6 to damage, which partially rescued Tg2576
428 mortality (30).

429 Besides mortality, weight loss is also a prominent clinical feature in AD, evident in
430 both human patients and transgenic mouse models (40). As previously reported
431 (30,41), a significant decrease in body weight was observed in Tg2576 mice. IL-6
432 has long been recognized for its significant role in central regulation of body weight,
433 energy balance, and body fat at the central level (42,43). In our study, IL-6-deficient
434 male mice also displayed late-onset obesity, consistent with these reports.
435 Accordingly, body weight was decreased in IL-6-overexpressing mice, further
436 supporting the role of IL-6 in body weight regulation. Interestingly, while IL-6 affected
437 body weight in wild-type animals, its effects were limited in Tg2576 mice, suggesting

438 that the specific effects of IL-6 on body weight regulation may be influenced and
439 altered within the Tg2576 setting.

440 The behavioral phenotype of Tg2576 mice has been broadly studied at different
441 stages of the disease, and it has been generally established that these mice display
442 age-related behavioral alterations at an early onset, including hyperactivity, increased
443 exploration, and decreased anxiety-like behavior, accompanied by a decline in
444 cognitive function (12,14,15,44–47). Our study successfully replicated these findings
445 in both young and aged mice, uncovering age-associated effects and sex-specific
446 variations. IL-6 signaling appears to modulate a variety of behaviors. Thus, previous
447 studies on IL-6-deficient mice have reported hypoactivity and decreased exploration
448 (19,21,29), despite some conflicting results have been reported (48). In our study, the
449 effects of IL-6 were mostly observed in Tg2576 rather than in wild-type mice,
450 regulating general activity and exploration. In young Tg2576 mice, IL-6
451 overexpression tended to potentiate hyperactivity and exploratory behavior, while IL-
452 6 deficiency tended to blunt activity without clear effects on exploration. Conversely,
453 in aged mice, both IL-6 overexpression and IL-6 deficiency tended to inhibit activity
454 and exploratory behavior in Tg2576 mice, and ultimately, in wild-type mice as well.
455 The anxiolytic-like effect of IL-6 has previously been described (49). IL-6
456 overexpression further decreased anxiety in both young and aged Tg2576 mice,
457 while IL-6 deficiency also decreased anxiety in aged Tg2576 female mice but
458 increased it in both Tg2576 and wild-type males. Accordingly, increased anxiety has
459 been previously reported in IL-6-deficient mice (19,20,29). These findings underscore
460 the potential role of IL-6 in modulating behavior and suggest that sex-specific
461 differences may contribute to IL-6-mediated effects.

462 In our study, Tg2576 mice exhibited impaired learning and memory compared to
463 age-matched controls. Remarkably, we identified sex-dependent differences in
464 cognitive performance, potentially indicating task sensitivity variations, as previously
465 reported by others (14). The cognitive impairment of Tg2576 mice has been found to
466 correlate with deficits in long-term potentiation (LTP) in the hippocampus (44,50).
467 Hippocampal-dependent learning and memory are significantly influenced by IL-6,
468 and studies have reported a negative association between IL-6 levels and cognitive
469 function (51,52). Interestingly, blocking endogenous IL-6 in a “healthy” brain has
470 proven to remarkably prolong LTP and enhance long-term memory in hippocampal-

471 dependent tasks (25,53). In our study, while IL-6 overexpression improved working
472 memory in Tg2576 mice, it had a cumulative negative effect on spatial reference
473 memory. Consistently, IL-6 deficiency enhanced spatial learning and memory. The
474 age-dependent effect of IL-6 on cognitive impairment had previously been reported
475 both in IL-6-deficient mice (54,55) and in IL-6-overexpressing mice (56), possibly
476 affected by the age-dependent neurologic pathology, reduced LTP, and reductions in
477 cerebellar volume (22,57). Collectively, our results suggest that IL-6 plays a pivotal
478 role in learning and memory processes, with effects influenced by factors such as
479 sex, age, cognitive task, and brain regions assessed. Disruptions in IL-6 signaling
480 may impact brain development and, consequently, brain functions (8,53,54).

481 Motor impairments are also a common late-onset symptom in AD patients, which
482 may be related to cognitive decline (58). Motor function abnormalities are observed in
483 studies performed in APP mouse models of AD, which have been attributed to a
484 cortical dysfunction in the processing of information induced by Aβ (14,45,59,60). In
485 line with this, our study revealed decreased motor coordination and balance in
486 Tg2576 mice. Moreover, our findings align with reports of progressive neurological
487 disease in GFAP-IL6 mice, characterized by ataxia, tremor, motor impairment,
488 seizures, and premature mortality (22,26). However, the effect of IL-6 on motor
489 performance in Tg2576 mice was moderate. Previous studies in various mouse
490 models of AD have also reported poor nesting performance, which may be influenced
491 by a combination of sensorimotor deficits, episodic memory issues, and hyperactivity
492 (46,61,62). Consistently, nesting behavior was significantly decreased in Tg2576
493 mice in our study. Interestingly, IL-6 deficiency improved the nesting scores in aged
494 mice, suggesting an age-dependent role for IL-6 in regulating distress.

495 Mutant hAPP overexpression in Tg2576 mice leads to the secretion of $A\beta_{42}$ and
496 $A\beta_{40}$ and to the formation of senile plaques with dense amyloid cores (12). In our
497 study, we confirmed the presence of full-length hAPP in the cortex and hippocampus
498 of Tg2576 mice. However, the findings regarding amyloid production presented
499 conflicting results, and are dependent on the specific Tg2576 founder mice
500 employed, as discussed below. In the IL-6 overexpression study, elevated levels of
501 Aβ were observed, as expected. It has been previously reported that the expression
502 of inflammatory mediators, including IL-6, could enhance APP expression and
503 processing and influence Aβ deposition, potentially establishing a positive feedback

504 loop that contributes to neurodegeneration (63,64). However, astrocytic IL-6
505 overexpression decreased APP and total Aβ peptides levels, with opposite effects on
506 $A\beta_{40}$ and $A\beta_{42}$ isoforms. Interestingly, increased levels of the most pathogenic $A\beta_{42}$
507 isoform were detected, thereby increasing the $A\beta_{42}/A\beta_{40}$ ratio and suggesting a
508 potential association with enhanced plaque deposition. Hence, IL-6 overexpression
509 tended to increase amyloid deposition, contrary to the findings in young TgCRND8
510 mice with AAV IL-6 overexpression (23).

511 Glial reactivity is a common feature of Tg2576 mice, occurring alongside amyloid
512 plaque deposition (3,4), and of GFAP-IL6 mice, which develop a progressive
513 neuroinflammatory state in the brain parenchyma due to the chronic production of
514 low levels of IL-6 in the brain (52). While gliosis was predominantly associated with
515 amyloid plaques in Tg2576 mice, astrocytic IL-6 overexpression dramatically
516 decreased the glial reactivity responding to amyloid plaques. This strongly suggests
517 an alteration in the physiological responses of glial cells to amyloid plaques in GFAP-
518 IL6 mice. Thus, the moderate increase in amyloid plaque load observed in IL-6-
519 overexpressing mice could be attributed to a potential overload of glial cell
520 phagocytic capacity, resulting in ineffective clearance. The microenvironment
521 surrounding amyloid plaques appears to be crucial in modulating glial cell phagocytic
522 function and influencing Aβ deposit clearance. Indeed, the heterogeneous nature of
523 microglial responses in the context of plaque formation has already been reported by
524 other studies (4,65). Finally, it is noteworthy that GFAP-IL6 mice display glial cell
525 reactivity at early stages mice (52), preceding plaque formation, which could
526 potentially affect the pattern observed in our mice.

527 Unexpectedly, in the IL-6 deficiency study, Aβ peptides and amyloid plaques were
528 notably absent in the neural tissue of Tg2576 and Tg2576/IL6KO mice, despite
529 normal levels of the precursor protein APP. It must be emphasized that the Tg2576
530 founder mice varied between the two studies. This discrepancy raised several
531 hypotheses, including genetic drift in the APP gene, impaired APP processing,
532 increased Aβ clearance or degradation, or interference with the genetic background
533 of IL-6-deficient mice. However, the latter seems unlikely, as both GFAP-IL6 and IL-
534 6KO mice share a similar background. Previous studies had reported that the APP
535 transgene, although being expressed at the highest level in the brain, is substantially
536 expressed in other organs as well. Nevertheless, the production of Aβ peptides

537 seems to be restricted to the brain (66). However, $A\beta_{40}$ and $A\beta_{42}$ were present in
538 serum samples and significantly decreased by IL-6 deficiency. Remarkably, our
539 Tg2576 mice, heterozygous for IL-6, exhibited reduced Aβ levels in contrast to
540 Tg2576 positive controls, homozygous for IL-6, suggesting a potential regulatory role
541 of IL-6 in modulating circulating Aβ levels. These results point to a potential
542 independent central or peripheral source of Aβ under the control of IL-6 that deserves
543 further attention. Interestingly, glial reactivity was also increased regardless of Aβ
544 production and accumulation in Tg2576 mice. IL-6 deficiency also induced a glial
545 response, possibly linked to the anti-inflammatory properties of this cytokine.
546 Therefore, the involvement of IL-6 in mediating responses to various stimuli
547 highlights the potential impact of IL-6 dysregulation on altered neuroinflammation in
548 the brain.

549 Despite the lack of abundant amyloidosis, similar physiological and behavioral
550 changes were observed, suggesting that these phenotypical traits of Tg2576 mice
551 may occur independently of significant amounts of Aβ. Prior research has established
552 that cognitive decline and impaired behavior in Tg2576 mice precede the deposition
553 of Aβ, emphasizing that plaque formation is not necessarily a prerequisite for
554 cognitive impairment (12,30,41,67). Consequently, the focus has shifted towards
555 alternative mechanisms beyond Aβ and its aggregated forms' toxicity, including
556 neurodevelopmental effects attributed to compensatory processes triggered by APP
557 overexpression, specific APP metabolites, and/or adjacent background genes
558 (67,68). In fact, APP and its family members play different roles during brain
559 development, maturity, and aging, impacting gene regulation and processes like cell
560 proliferation and neurogenesis (69). APP involvement in synapse formation and
561 neural networks from early stages suggests its key role in maintaining robust brain
562 circuits. Disruptions in APP signaling may lead to genetic-dependent dysregulation of
563 synapse dynamics and cellular signaling, contributing to cognitive alterations
564 independently of Aβ toxicity. Thus, Aβ alone may be sufficient, but not necessary, for
565 the development of AD pathology (18,70). Additionally, intracellular APP fragments
566 including C99 significantly contribute to the early pathological events and to the
567 initiation of the neurodegenerative process in AD (16).

568 Taken together, our data provides a novel perspective on the potential
569 contribution of APP, rather than Aβ, in the pathological manifestations observed in

570 Tg2576 mice. Previous unsuccessful attempts to develop therapeutic approaches for
571 AD targeting Aβ dysregulation already suggest that while Aβ may contribute to the
572 pathogenesis of AD, it is not sufficient to cause cognitive decline or impairments in
573 global functioning (16,71). Furthermore, our findings highlight the multifaceted nature
574 of IL-6 in physiological and neurodegenerative disorders as AD. The implication of IL-
575 6 in the early stages of the disease suggests that addressing IL-6 dyshomeostasis
576 could be an effective strategy for managing symptoms during the early stages of the
577 disease.

578

579 **6. Conclusions**

580 - The study demonstrates that IL-6 plays a complex role in Tg2576 mice, with
581 varying effects on survival, body weight, behavior, and cognition.
582 - Contrary to expectations, many observed physiological and behavioral
583 changes in Tg2576 mice seem to occur independently of significant APP
584 processing, Aβ peptide production, or amyloid plaque deposition.
585 - CNS-specific IL-6 overexpression modulates glial reactivity surrounding
586 amyloid plaques in Tg2576 mice.

587

588 **7. Declarations**

589 **Ethics approval**

590 All experimental protocols were approved by the Ethics Committee on Animal and
591 Human Experimentation (CEEAH) of the Autonomous University of Barcelona (3971
592 and 9861) and were conducted in accordance with the Spanish legislation and the
593 EU directive (2010/63/UE) on 'Protection of Animals Used for Experimental and
594 Other Scientific Purposes'.

595 **Consent for publication**

596 Not applicable.

597 **Availability of data and materials**

598 The data that support the findings of this study are available from the corresponding
599 author upon reasonable request.

600

Competing interests

The authors claim no competing interests.

Funding

This study was supported by Ministerio de Economía y Competitividad y Fondo Europeo de Desarrollo Regional SAF2014-56546-R; Ministerio de Ciencia, Innovación y Universidades y Fondo Europeo de Desarrollo Regional RTI2018-101105-B-I00; and Ministerio de Ciencia e Innovación y Fondo Europeo de Desarrollo Regional PID2021-126602OB-I00.

Authors' contributions

C.C. and J.H. conceived and designed the study. C.C., K.A., G.C., P.S, M.G., and A.M performed research. C.C. performed the formal analysis of the data. C.C. and J.H. wrote the initial draft of the manuscript. All authors edited and reviewed the manuscript.

Acknowledgements

The GFAP-IL6 mice were obtained from The Scripps Research Institute (La Jolla, USA) where they were developed by I. L. Campbell (28). C.C. and K.A. acknowledge the support of PIF UAB and FPU17/02065 fellowships, respectively. P.S. received the Lundbeck R380-2021-1300 fellowship.

8. References

1. Long JM, Holtzman DM. Alzheimer disease: an update on pathobiology and treatment strategies. Cell. 2019 Oct 3;179(2):312–39.
2. Knopman DS, Amieva H, Petersen RC, Chételat G, Holtzman DM, Hyman BT, et al. Alzheimer disease. Nat Rev Dis Primers. 2021 Dec 1;7(1).
3. Heneka MT, Carson MJ, El Khoury J, Landreth GE, Brosseron F, Feinstein DL, et al. Neuroinflammation in Alzheimer's disease. Lancet Neurol. 2015;14(4):388–405.
4. Frautschy SA, Yang F, Irrizarry M, Hyman B, Saido TC, Hsiao K, et al. Microglial response to amyloid plaques in APPsw transgenic mice. Am J Pathol. 1998;152(1):307–17.
5. Glass CK, Saijo K, Winner B, Marchetto MC, Gage FH. Mechanisms underlying inflammation in neurodegeneration. Cell. 2010;140(6):918–34.
6. Saito T, Saido TC. Neuroinflammation in mouse models of Alzheimer's disease. Clin Exp Neuroimmunol. 2018 Nov 1;9(4):211–8.
7. Calsolaro V, Edison P. Neuroinflammation in Alzheimer's disease: current evidence and future directions. Alzheimers Dement. 2016 Jun 1;12(6):719–32.
8. Erta M, Quintana A, Hidalgo J. Interleukin-6, a major cytokine in the central nervous system. Int J Biol Sci. 2012;8(9):1254–66.
9. Hüll M, Strauss S, Berger M, Volk B, Bauer J. The participation of interleukin-6, a stress-inducible cytokine, in the pathogenesis of Alzheimer's disease. Behav Brain Res. 1996;78(1):37–41.
10. Sastre M, Dewachter I, Landreth GE, Willson TM, Klockgether T, Van Leuven F, et al. Nonsteroidal anti-inflammatory drugs and peroxisome proliferator-activated receptor-γ agonists modulate immunostimulated processing of amyloid precursor protein through regulation of β-secretase. J Neurosci. 2003;23(30):9796–804.
11. Apelt J, Schliebs R. β-Amyloid-induced glial expression of both pro- and anti-inflammatory cytokines in cerebral cortex of aged transgenic Tg2576 mice with Alzheimer plaque pathology. Brain Res. 2001;894(1):21–30.
12. Hsiao K, Chapman P, Nilsen S, Eckman C, Harigaya Y, Younkin S, et al. Correlative memory deficits, Aβ elevation, and amyloid plaques in transgenic mice. Science (1979). 1996;274(5284):99–102.
13. Westerman MA, Cooper-Blacketer D, Mariash A, Kotilinek L, Kawarabayashi T, Younkin LH, et al. The relationship between Aβ and memory in the Tg2576 mouse model of Alzheimer's disease. J Neurosci. 2002;22(5):1858–67.
14. King DL, Arendash GW. Behavioral characterization of the Tg2576 transgenic model of Alzheimer's disease through 19 months. Physiol Behav. 2002;75(5):627–42.
15. Ognibene E, Middei S, Daniele S, Adriani W, Ghirardi O, Caprioli A, et al. Aspects of spatial memory and behavioral disinhibition in Tg2576 transgenic mice as a model of Alzheimer's disease. Behav Brain Res. 2005 Jan 30;156(2):225–32.
16. Checler F, Afram E, Pardossi-Piquard R, Lauritzen I. Is γ-secretase a beneficial inactivating enzyme of the toxic APP C-terminal fragment C99? J Biol Chem. 2021 Jan 1;296.
17. Höfling C, Shehabi E, Kuhn PH, Lichtenthaler SF, Hartlage-Rübsamen M, Roßner S. Cell type-specific human APP transgene expression by hippocampal interneurons in the Tg2576 mouse model of Alzheimer's disease. Front Neurosci. 2019;13.
18. Dourlen P, Kilinc D, Malmanche N, Chapuis J, Lambert JC. The new genetic landscape of Alzheimer's disease: from amyloid cascade to genetically driven synaptic failure hypothesis? Acta Neuropathol. 2019 Aug 1;138(2):221–36.
19. Armario A, Hernandez J, Bluethmann H, Hidalgo J. IL-6 deficiency leads to increased emotionality in mice: evidence in transgenic mice carrying a null mutation for IL-6. J Neuroimmunol. 1998;92(1–2):160–9.

680 20. Butterweck V, Prinz S, Schwaninger M. The role of interleukin-6 in stress-induced
681 hyperthermia and emotional behaviour in mice. Behav Brain Res. 2003 Sep 15;144(1–2):49–
682 56.
683 21. Baier PC, May U, Scheller J, Rose-John S, Schiffelholz T. Impaired hippocampus-dependent
684 and -independent learning in IL-6 deficient mice. Behav Brain Res. 2009 Jun 8;200(1):192–6.
685 22. Gyengesi E, Rangel A, Ullah F, Liang H, Niedermayer G, Asgarov R, et al. Chronic microglial
686 activation in the GFAP-IL6 mouse contributes to age-dependent cerebellar volume loss and
687 impairment in motor function. Front Neurosci. 2019;13:1–14.
688 23. Chakrabarty P, Jansen-West K, Beccard A, Ceballos-Diaz C, Levites Y, Verbeeck C, et al.
689 Massive gliosis induced by interleukin-6 suppresses Aβ deposition in vivo: evidence against
690 inflammation as a driving force for amyloid deposition. FASEB J. 2010 Feb;24(2):548–59.
691 24. Rothaug M, Becker-Pauly C, Rose-John S. The role of interleukin-6 signaling in nervous tissue.
692 Biochim Biophys Acta Mol Cell Res. 2016 Jun 1;1863(6):1218–27.
693 25. Lyra e Silva NM, Gonçalves RA, Pascoal TA, Lima-Filho RAS, Resende E de PF, Vieira ELM,
694 et al. Pro-inflammatory interleukin-6 signaling links cognitive impairments and peripheral
695 metabolic alterations in Alzheimer's disease. Transl Psychiatry. 2021 Jun 1;11(2).
696 26. Campbell IL, Abraham CR, Masliah E, Kemper P, Inglis JD, Oldstone MBA, et al. Neurologic
697 disease induced in transgenic mice by cerebral overexpression of interleukin 6. Proc Natl Acad
698 Sci USA. 1993;90(21):10061–5.
699 27. Sanchis P, Fernández-Gayol O, Comes G, Aguilar K, Escrig A, Giralt M, et al. A new mouse
700 model to study restoration of interleukin-6 (IL-6) expression in a Cre-dependent manner:
701 microglial IL-6 regulation of experimental autoimmune encephalomyelitis. J Neuroinflammation.
702 2020 Dec 1;17(1).
703 28. Hsiao KK, Borchelt DR, Olson K, Johannsdottir R, Kitt C, Yunis W, et al. Age-related CNS
704 disorder and early death in transgenic FVB/N mice overexpressing Alzheimer amyloid
705 precursor proteins. Vol. 15, Neuron. 1995. p. 1203–18.
706 29. Erta M, Giralt M, Esposito FL, Fernandez-Gayol O, Hidalgo J. Astrocytic IL-6 mediates
707 locomotor activity, exploration, anxiety, learning and social behavior. Horm Behav. 2015 Jul
708 1;73:64–74.
709 30. Escrig A, Canal C, Sanchis P, Fernández-Gayol O, Montilla A, Comes G, et al. IL-6 trans-
710 signaling in the brain influences the behavioral and physio-pathological phenotype of the
711 Tg2576 and 3xTgAD mouse models of Alzheimer's disease. Brain Behav Immun. 2019 Nov
712 1;82:145–59.
713 31. Deacon RMJ. Assessing nest building in mice. Nat Protoc. 2006 Aug;1(3):1117–9.
714 32. Schneider CA, Rasband WS, Eliceiri KW. NIH Image to ImageJ: 25 years of image analysis.
715 Vol. 9, Nature Methods. 2012. p. 671–5.
716 33. Su F, Bai F, Zhang Z. Inflammatory cytokines and Alzheimer's disease: a review from the
717 perspective of genetic polymorphisms. Neurosci Bull. 2016 Oct 1;32(5):469–80.
718 34. Leissring MA, Farris W, Chang AY, Walsh DM, Wu X, Sun X, et al. Enhanced proteolysis of β-
719 amyloid in APP transgenic mice prevents plaque formation, secondary pathology, and
720 premature death. Neuron. 2003;40(6):1087–93.
721 35. Carlson GA, Borchelt DR, Dake A, Turner S, Danielson V, Coffin JD, et al. Genetic modification
722 of the phenotypes produced by amyloid precursor protein overexpression in transgenic mice.
723 Hum Mol Genet. 1997;6(11):1951–9.
724 36. Krezowski J, Knudson D, Ebeling C, Pitstick R, Giri RK, Schenk D, et al. Identification of loci
725 determining susceptibility to the lethal effects of amyloid precursor protein transgene
726 overexpression. Hum Mol Genet. 2004 Sep 15;13(18):1989–97.
727 37. Rae EA, Brown RE. The problem of genotype and sex differences in life expectancy in
728 transgenic AD mice. Neurosci Biobehav Rev. 2015 Oct 1;57:238–51.

38. Westmark CJ, Westmark PR, Beard AM, Hildebrandt SM, Malter JS. Seizure susceptibility and mortality in mice that over-express amyloid precursor protein. Int J Clin Exp Pathol. 2008;1(2):157–68.
39. Abbott NJ, Rönnbäck L, Hansson E. Astrocyte-endothelial interactions at the blood-brain barrier. Nat Rev Neurosci. 2006 Jan;7(1):41–53.
40. Gillette-Guyonnet S, Nourhashémi F, Andrieu S, de Glisezinski I, Ousset PJ, Rivière D, et al. Weight loss in Alzheimer disease. Am J Clin Nutr. 2000;71(2):637–42.
41. Manso Y, Carrasco J, Comes G, Meloni G, Adlard PA, Bush AI, et al. Characterization of the role of metallothionein-3 in an animal model of Alzheimer's disease. Cell Mol Life Sci. 2012 Nov;69(21):3683–700.
42. Wallenius V, Wallenius K, Ahrén B, Rudling M, Carlsten H, Dickson SL, et al. Interleukin-6-deficient mice develop mature-onset obesity. Nat Med. 2002;8(1):75–9.
43. Señarís RM, Trujillo ML, Navia B, Comes G, Ferrer B, Giralt M, et al. Interleukin-6 regulates the expression of hypothalamic neuropeptides involved in body weight in a gender-dependent way. J Neuroendocrinol. 2011 Aug;23(8):675–86.
44. Chapman PF, White GL, Jones MW, Cooper-Blacketer D, Marshall VJ, Irizarry M, et al. Impaired synaptic plasticity and learning in aged amyloid precursor protein transgenic mice. Nat Neurosci. 1999;2(3):271–6.
45. Lalonde R, Lewis TL, Strazielle C, Kim H, Fukuchi K. Transgenic mice expressing the βAPP695SWE mutation: effects on exploratory activity, anxiety, and motor coordination. Brain Res. 2003 Jul 4;977(1):38–45.
46. Deacon RMJ, Cholerton LL, Talbot K, Nair-Roberts RG, Sanderson DJ, Romberg C, et al. Age-dependent and -independent behavioral deficits in Tg2576 mice. Behav Brain Res. 2008 May 16;189(1):126–38.
47. Reed MN, Liu P, Kotilinek LA, Ashe KH. Effect size of reference memory deficits in the Morris water maze in Tg2576 mice. Behav Brain Res. 2010 Sep;212(1):115–20.
48. Swiergiel AH, Dunn AJ. Feeding, exploratory, anxiety-and depression-related behaviors are not altered in interleukin-6-deficient male mice. Behav Brain Res. 2006;171(1):94–108.
49. Wei H, Chadman KK, McCloskey DP, Sheikh AM, Malik M, Brown WT, et al. Brain IL-6 elevation causes neuronal circuitry imbalances and mediates autism-like behaviors. Biochim Biophys Acta. 2012 Jun;1822(6):831–42.
50. Huh S, Baek SJ, Lee KH, Whitcomb DJ, Jo J, Choi SM, et al. The reemergence of long-term potentiation in aged Alzheimer's disease mouse model. Sci Rep. 2016 Jul 5;6.
51. Boulanger LM. Immune proteins in brain development and synaptic plasticity. Neuron. 2009 Oct 15;64(1):93–109.
52. Campbell IL, Hofer MJ, Pagenstecher A. Transgenic models for cytokine-induced neurological disease. Biochim Biophys Acta. 2010 Oct;1802(10):903–17.
53. Balschun D, Wetzel W, Del Rey A, Pitossi F, Schneider H, Zuschratter W, et al. Interleukin-6: a cytokine to forget. FASEB J. 2004 Nov;18(14):1788–90.
54. Braida D, Sacerdote P, Panerai AE, Bianchi M, Aloisi AM, Iosuè S, et al. Cognitive function in young and adult IL (interleukin)-6 deficient mice. Behav Brain Res. 2004 Aug 31;153(2):423–9.
55. Bialuk I, Winnicka MM. Facilitatory effect of IL-6 deficiency on long-term spatial memory in young adult mice. Behav Genet. 2018 May 1;48(3):236–46.
56. Chesworth R, Gamage R, Ullah F, Sonego S, Millington C, Fernandez A, et al. Spatial memory and microglia activation in a mouse model of chronic neuroinflammation and the anti-inflammatory effects of apigenin. Front Neurosci. 2021 Jul 30;15.
57. Steffensen SC, Campbell IL, Henriksen SJ. Site-specific hippocampal pathophysiology due to cerebral overexpression of interleukin-6 in transgenic mice. Brain Res. 1994;652:149–53.
58. Buchman AS, Bennett DA. Loss of motor function in preclinical Alzheimer's disease. Expert Rev Neurother. 2011 May;11(5):665–76.

59. Lalonde R, Fukuchi KI, Strazielle C. Neurologic and motor dysfunctions in APP transgenic mice. Rev Neurosci. 2012 Aug;23(4):363–79.
60. Nyul-Toth A, DelFavero J, Mukli P, Tarantini A, Ungvari A, Yabluchanskiy A, et al. Early manifestation of gait alterations in the Tg2576 mouse model of Alzheimer's disease. Geroscience. 2021 Aug 1;43(4):1947–57.
61. Filali M, Lalonde R. Age-related cognitive decline and nesting behavior in an APPswe/PS1 bigenic model of Alzheimer's disease. Brain Res. 2009 Sep 25;1292:93–9.
62. Wesson DW, Wilson DA. Age and gene overexpression interact to abolish nesting behavior in Tg2576 amyloid precursor protein (APP) mice. Behav Brain Res. 2011 Jan 1;216(1):408–13.
63. Brugg B, Dubreuil YL, Hubert G, Wollmant EE, Delhaye-Bouchaud N, Mariani J. Inflammatory processes induce β-amyloid precursor protein changes in mouse brain. Proc Natl Acad Sci USA. 1995;92(7):3032–5.
64. Griffin WST, Sheng JG, Royston MC, Gentleman SM, McKenzie JE, Graham DI, et al. Glial-neuronal interactions in Alzheimer's disease: the potential role of a 'cytokine cycle' in disease progression. Brain Pathol. 1998;8(1):65–72.
65. Gyoneva S, Swanger SA, Zhang J, Weinshenker D, Traynelis SF. Altered motility of plaque-associated microglia in a model of Alzheimer's disease. Neuroscience. 2016 Aug 25;330:410–20.
66. Kawarabayashi T, Younkin LH, Saido TC, Shoji M, Ashe KH, Younkin SG. Age-dependent changes in brain, CSF, and plasma amyloid protein in the Tg2576 transgenic mouse model of Alzheimer's disease. J Neurosci. 2001;21(2):372–81.
67. King DL, Arendash GW, Crawford F, Sterk T, Menendez J, Mullan MJ. Progressive and gender-dependent cognitive impairment in the APPSW transgenic mouse model for Alzheimer's disease. Behav Brain Res. 1999;103:145–62.
68. Johnson ECB, Ho K, Yu GQ, Das M, Sanchez PE, Djukic B, et al. Behavioral and neural network abnormalities in human APP transgenic mice resemble those of App knock-in mice and are modulated by familial Alzheimer's disease mutations but not by inhibition of BACE1. Mol Neurodegener. 2020 Dec 1;15(1).
69. Zhang YW, Thompson R, Zhang H, Xu H. APP processing in Alzheimer's disease. Mol Brain. 2011;4(3).
70. Priller C, Bauer T, Mitteregger G, Krebs B, Kretzschmar HA, Herms J. Synapse formation and function is modulated by the amyloid precursor protein. J Neurosci. 2006;26(27):7212–21.
71. Sun BL, Li WW, Zhu C, Jin WS, Zeng F, Liu YH, et al. Clinical research on Alzheimer's disease: progress and perspectives. Neurosci Bull. 2018 Dec 1;34(6):1111–8.

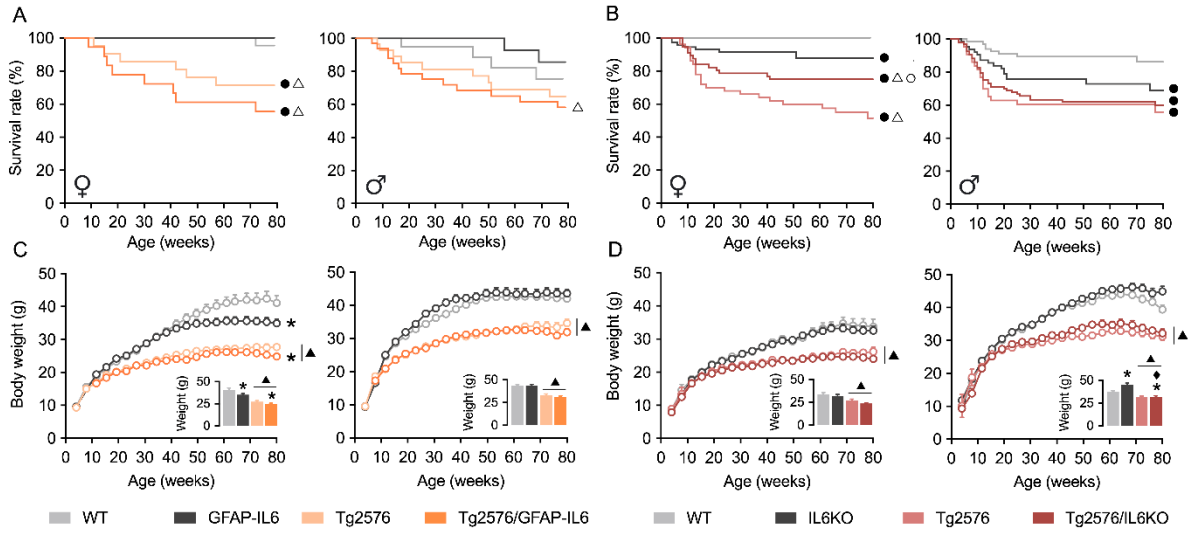

Figure 1. Effect of IL-6 on life span and body weight of Tg2576 mice. Kaplan-Meier survival curves for the IL-6 overexpression study (A) and for the IL-6 deficiency study (B). Results are analyzed by log-rank test; ● $p \leq .05$ vs WT, △ $p \leq .05$ vs GFAP-IL6 or IL6KO, ○ $p \leq .05$ vs Tg2576. Body weight curves and body weight at euthanasia (inset) for the IL-6 overexpression study (C) and for the IL-6 deficiency study (D). Results are mean ± SEM and analyzed by GEE and GzLM statistical tests; ▲ $p \leq .05$ Tg2576 effect, * $p \leq .05$ IL-6 effect. n = 18 - 30 in females, n = 20 - 38 in males at 3 weeks; n = 11 - 30 in females, n = 14 - 26 in males at 80 weeks for the IL-6 overexpression study; n = 51 - 72 in females, n = 51 - 67 in males at 3 weeks; n = 20 - 33 in females, n = 13 - 26 in males at 80 weeks for the IL-6 deficiency study.

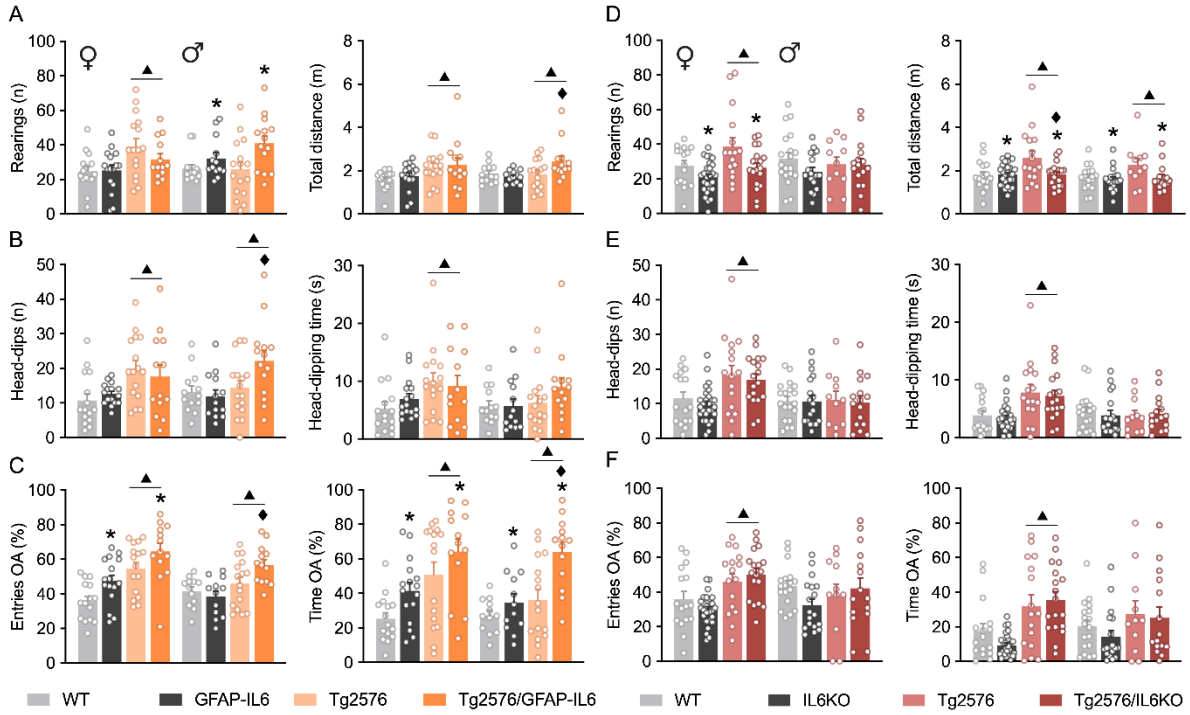

Figure 2. Impact of IL-6 on behavior of young Tg2576 mice. Number of rearings and total distance travelled in the OF test (A), number and time of head-dipping events in the HB test (B), and percentages of entries and time in the OA in the EPM test (C) of the IL-6 overexpression study, OA open arms. Similar results are represented for the IL-6 deficiency study in the OF, HB and EPM tests (D-F). Results are mean ± SEM and analyzed by GzLM statistical test; ▲ $p \leq .05$ Tg2576 effect, * $p \leq .05$ IL-6 effect, ♦ $p \leq .05$ interaction between both factors. n = 13 - 16 in females, n = 13 - 16 in males (A-C); n = 16 - 27 in females, n = 12 - 19 in males (D-F).

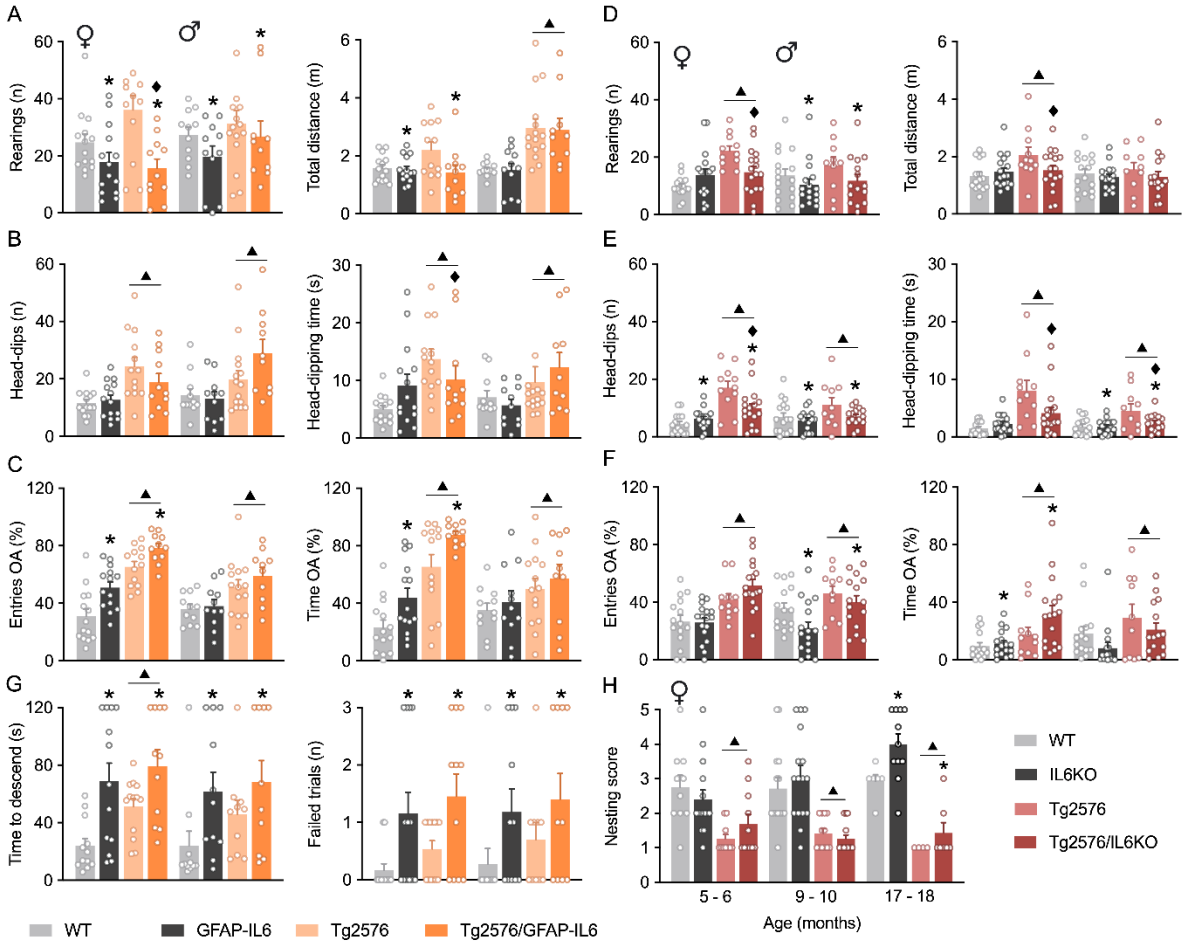

Figure 3. Impact of IL-6 on behavior of aged Tg2576 mice. Number of rearings and total distance travelled in the OF test (A), number and time of head-dipping events in the HB test (B), and percentages of entries and time in the OA in the EPM test (C) in the IL-6 overexpression study, OA open arms. Similar results are represented for the IL-6 deficiency study in the OF, HB and EPM tests (D-F). Time to descend and number of failed trials in the pole test in the IL-6 overexpression study (G). Nest-building scores for females in the IL-6 overexpression study (H). Results are mean ± SEM and analyzed by GzLM statistical test; ▲ $p \leq .05$ Tg2576 effect, * $p \leq .05$ IL-6 effect, ♦ $p \leq .05$ interaction between both factors. n = 11 - 14 in females, n = 10 - 15 in males (A-C); n = 11 - 17 in females, n = 10 - 16 in males (D-F); n = 10 - 13 in females, n = 10 - 11 in males (G); n = 5 - 16 (H).

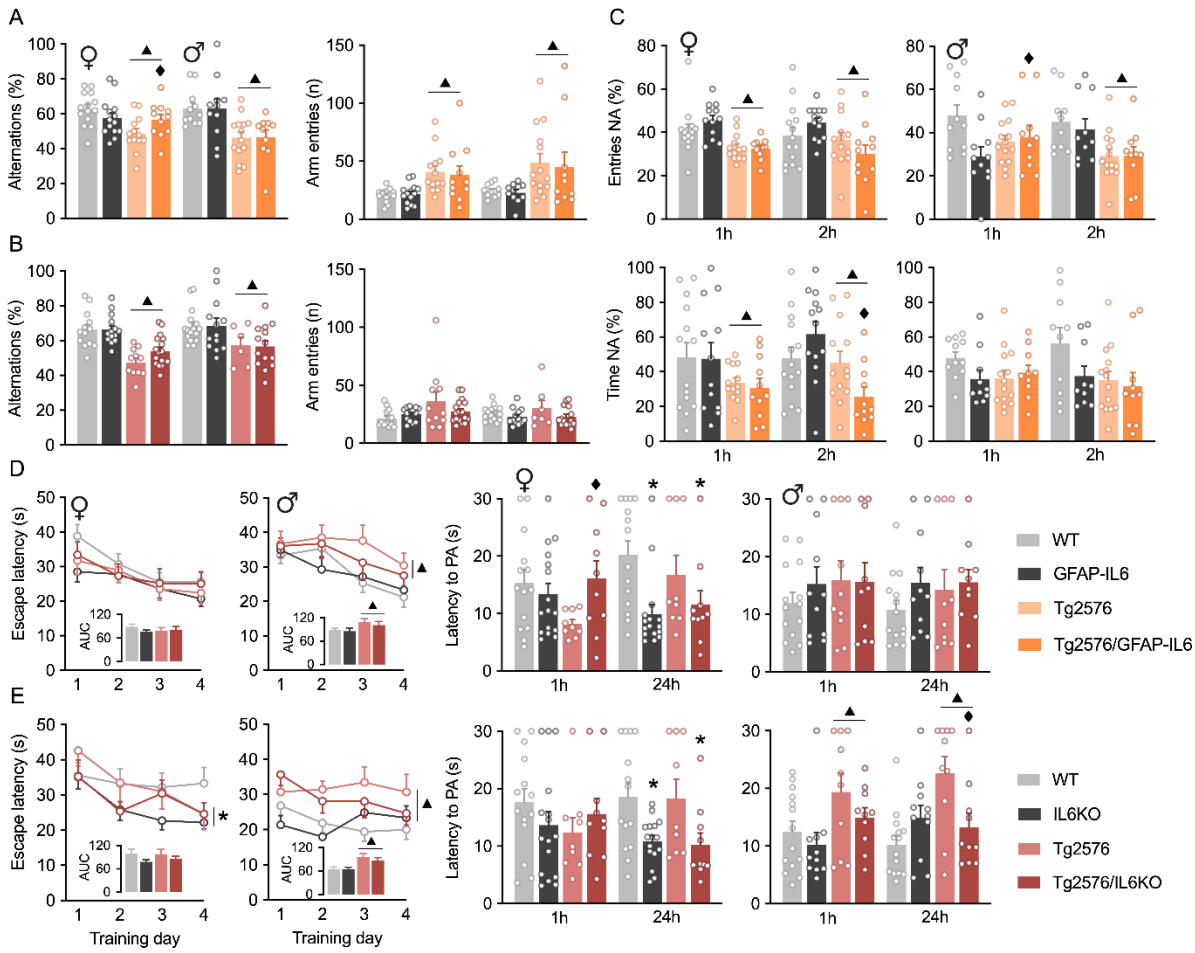

Figure 4. Effect of IL-6 on working and spatial memory of Tg2576 mice. Percentage of alternations and number of total arm entries in the YM test in the IL-6 overexpression study (A) and in the IL-6 deficiency study. Entries and time in the NA of the spatial memory YM test in the IL-6 overexpression study (C), NA novel arm. Spatial acquisition (D, left) and reversal (E, left) curves, with respective AUC quantifications (inset). Latency to PA in the probe trials of spatial acquisition (D, right) and reversal (E, right) phases at 1 h and 24 h of the MWM test in the IL-6 deficiency study, PA platform area. Results are mean ± SEM and analyzed by GzLM and GEE statistical tests; ▲ $p \leq .05$ Tg2576 effect, * $p \leq .05$ IL-6 effect, ♦ $p \leq .05$ interaction between both factors. n = 13 - 16 in females, n = 13 - 14 in males (A); n = 11 - 16 in females, n = 10 - 16 in males (B); n = 9 - 14 in females, n = 8 - 10 in males (C); n = 9 - 16 in females, n = 10 - 14 in males (D).

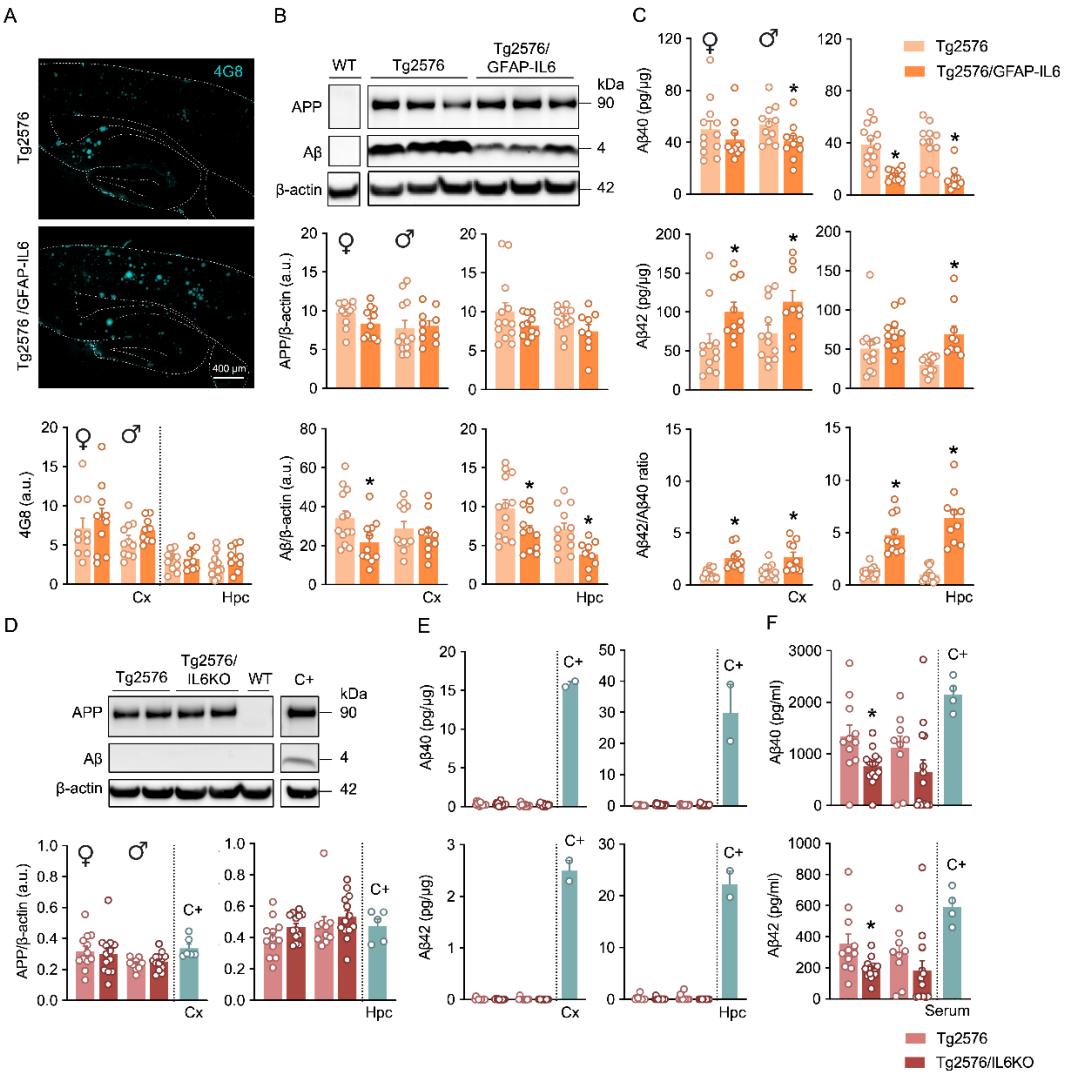

Figure 5. Effect of IL-6 on amyloidosis of Tg2576 mice. (A) Representative immunofluorescence of 4G8 and quantification of 4G8 levels in the Cx and Hpc of the IL-6 overexpression study (A). Representative immunoblot of 6E10 and quantification of APP and Aβ levels relative to β-actin in the Cx and Hpc in the IL-6 overexpression study (B). Aβ40 and Aβ42 levels in the Cx and Hpc, and relative Aβ42 / Aβ40 levels in the IL-6 overexpression study (C). Representative immunoblot of 6E10 and quantification of APP levels relative to β-actin in the Cx and Hpc of the IL-6 deficiency study (D). Aβ40 and Aβ42 levels in Cx and Hpc in the IL-6 deficiency study. (F) Aβ40 and Aβ42 levels in serum samples in the IL-6 deficiency study. Results are mean ± SEM and analyzed by Student's t-test; * $p \leq .05$ IL-6 effect. Cx cortex, Hpc hippocampus.

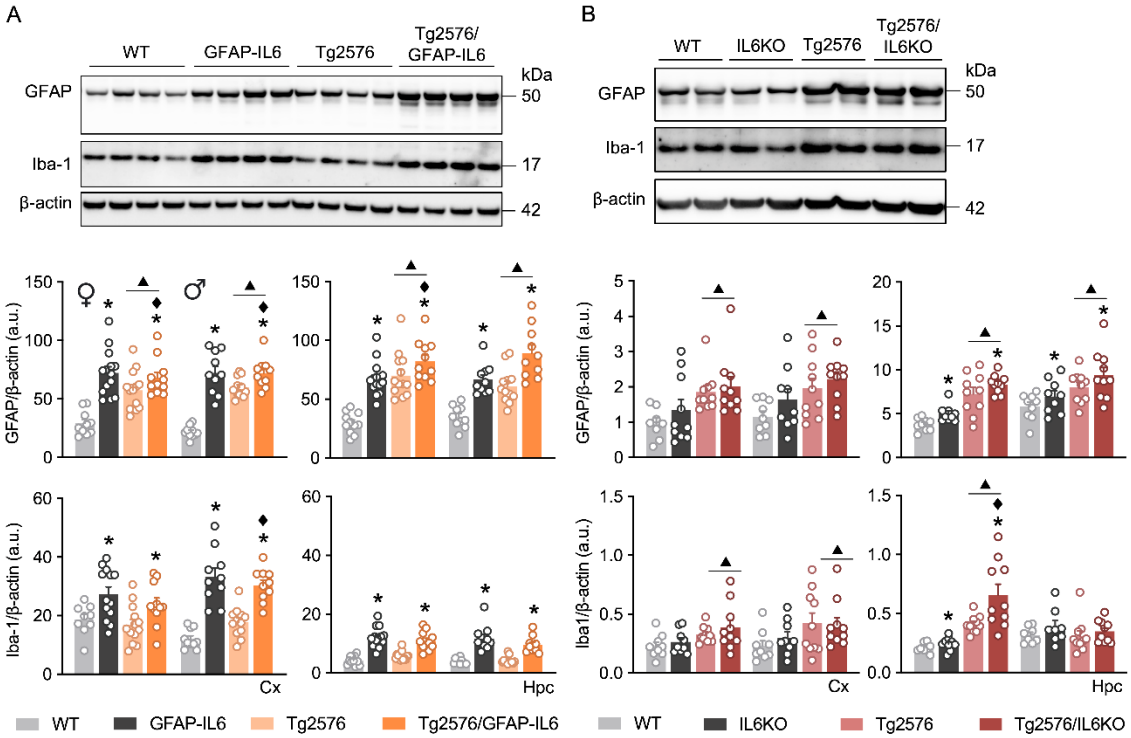

Figure 6. Effect of IL-6 on gliosis of Tg2576 mice. (A) Representative immunoblot of GFAP and Iba1 in Cx, and quantification of GFAP and Iba1 levels in Tg2576 mice relative to β-actin in Cx and Hpc in the IL-6 overexpression study. (B) Representative immunoblot of GFAP and Iba-1 in Cx, and quantification of GFAP and Iba1 levels in Tg2576 mice relative to β-actin in Cx and Hpc in the IL-6 deficiency study. Results are mean ± SEM and analyzed by GzLM statistical test; ▲ $p \leq .05$ Tg2576 effect, * $p \leq .05$ IL-6 effect, ♦ $p \leq .05$ interaction between both factors. Cx cortex, Hpc hippocampus.

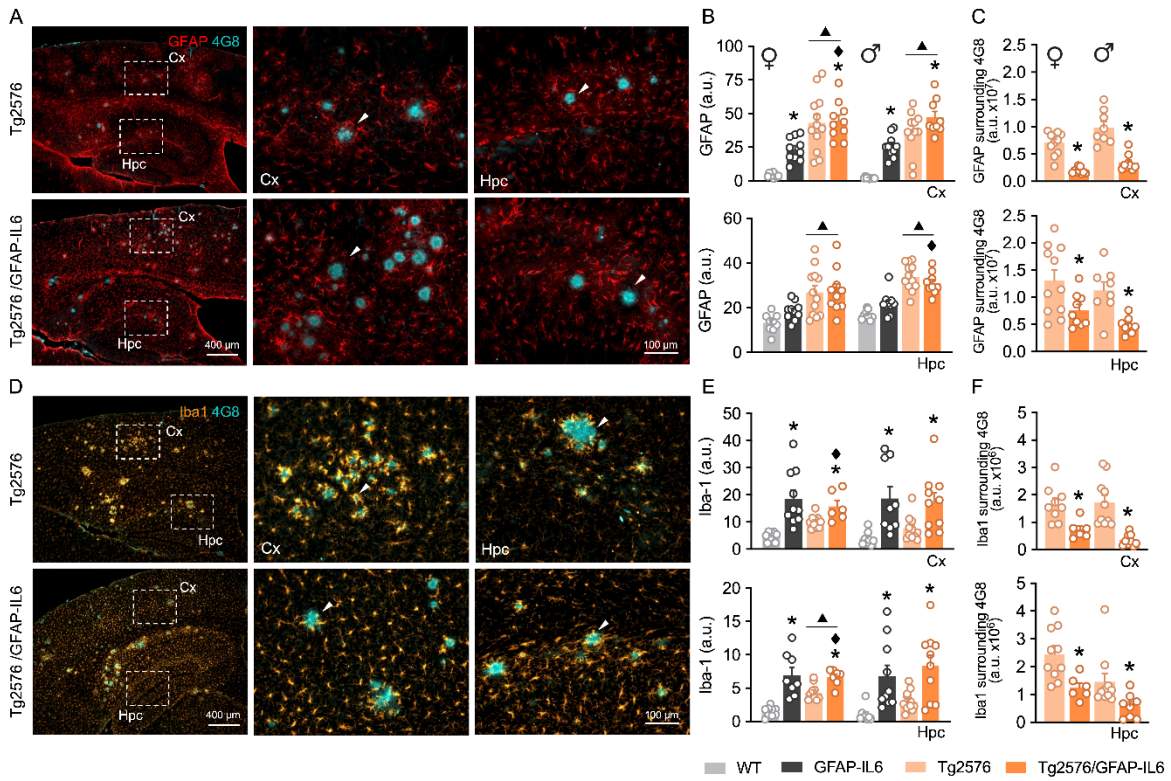

Figure 7. Effect of IL-6 overexpression on gliosis surrounding amyloid plaques of Tg2576 mice. (A) Representative immunostaining of GFAP and 4G8, higher magnifications of Cx (middle) and Hpc (right). (B) Quantification of GFAP levels in the Cx and Hpc. (C) Analysis of the percentage of GFAP surrounding amyloid plaques in the Cx and Hpc of Tg2576 mice. (D) Representative immunostaining of Iba1 and 4G8, higher magnifications of Cx (middle) and Hpc (right). (E) Quantification of Iba1 levels in the Cx and Hpc. (C) Analysis of the percentage of Iba1 surrounding amyloid plaques in the Cx and Hpc of Tg2576 mice. Results are mean ± SEM and analyzed by GzLM statistical test; ▲ $p \leq .05$ Tg2576 effect, * $p \leq .05$ IL-6 effect, ♦ $p \leq .05$ interaction between both factors. Cx cortex, Hpc hippocampus.